



Multiple bonding modes exhibited by heteroscorpionate N₂S(alkylthiolate) ligands with Zn(II) and Fe(II)

Vivek V. Karambelkar^a, Robert C. diTargiani^a, Christopher D. Incarvito^b, Lev N. Zakharov^c, Arnold L. Rheingold^c, Charlotte L. Stern^d, David P. Goldberg^{a,*}

^a Department of Chemistry, Johns Hopkins University, Baltimore, MD 21218, USA

^b Department of Chemistry, Yale University, New Haven, CT 06520-8107, USA

^c Department of Chemistry and Biochemistry, University of California, San Diego, CA 92093, USA

^d X-ray Crystallography Facility, Northwestern University, Evanston, IL 60208, USA

Received 9 July 2003; accepted 20 August 2003

Abstract

Two related heteroscorpionate N₂S(thiolate) ligands L¹ and L² have been employed in the synthesis of new zinc(II) and iron(II) complexes. These ligands contain two imidazolyl donors and one alkylthiolate donor connected by a central carbon atom. The ligand L¹ was reacted with ZnBr₂ to give the trinuclear zinc complex [(L¹)₃Zn₃Br₂]Br (**1**). The X-ray structure of **1** reveals one of the zinc ions to be coordinated by two L¹ ligands in a tripodal arrangement resulting in a distorted octahedral geometry, while the other two zinc ions are both held in a distorted tetrahedral geometry and are coordinated to another molecule of L¹ in an unusual tridentate, multibridging coordination mode. Modification of L¹ to include phenyl substituents on the imidazole groups leads to L², and these substituents cause quite a different result to be obtained in the reaction with ZnBr₂. The combination of L² and ZnBr₂ leads to the dimeric zinc complex (L²)₂Zn₂Br₂, (**2**). Characterization of **2** by X-ray diffraction shows this complex to be a dimer with a central Zn₂(μ-SR)₂ rhomb. Each zinc ion is found in a distorted tetrahedral geometry coordinated by L² in a bidentate, N,S fashion. The ¹H NMR spectrum of **2** provides strong evidence this structure is retained in solution. In comparison, reaction of L² with FeCl₂ leads to the monomeric complex (L²)₂Fe^{II} (**3**), which has each ligand coordinated in the same bidentate, N,S bonding mode. Interestingly, the methoxy groups of the two ligands in **3** are close enough to the iron center for a possible bonding interaction, suggesting an unexpected N₂O coordination mode.

© 2003 Elsevier Ltd. All rights reserved.

Keywords: Heteroscorpionate; Tripodal; Alkylthiolate; Imidazole; Iron; Zinc

1. Introduction

A variety of metalloproteins rely on a single metal ion cofactor bound to the protein by a combination of His_xCys_y amino acid ligands. Examples include zinc proteins such as the matrix metalloproteinases [1], zinc fingers [2], alcohol dehydrogenase [3], farnesyl transferase [4] and spinach carbonic anhydrase [5], as well as the blue copper proteins [6] and the non-heme iron enzymes nitrile hydratase [7] and peptide deformylase (PDF) [8].

We have specifically targeted the metal active site of the latter enzyme for synthetic modeling because we find it especially intriguing from an inorganic point of view; it utilizes an iron(II) center *in vivo* yet belongs to the mononuclear zinc(II) enzyme family in terms of both structure and function [8b]. In order to mimic the active site of PDF, which has a His₂Cys donor set coordinated to an M(II) ion in all of its known derivatives (M(II) = Fe(II), Zn(II), Co(II), Ni(II)), we have made efforts to synthesize ligands with mixed nitrogen/alkylthiolate donor sets. Accordingly, we recently prepared a simple linearly disposed N₂S(thiolate) ligand called PATH, which has led to the synthesis of a novel series of

* Corresponding author.

E-mail address: dpg@jhu.edu (D.P. Goldberg).

monomeric, pseudotetrahedral N_2S (thiolate) complexes ((PATH) $M^{II}L$; $M = Zn, Co$) [9–11]. These complexes have served as structural models for the generalized $(His)_2(Cys)M^{II}L$ active site of PDF, and recently we have shown that a PATH-Zn(II) complex generated in water acts as a functional model complex by catalyzing the hydrolysis of an ester substrate [12].

At the same time, we have also pursued the construction of scorpionate ligands bearing an N_2S (thiolate) donor set. The tris(pyrazolyl)borate (Tp) family of scorpionate ligands has proven remarkably useful for the construction of many enzyme model complexes, especially models of the zinc enzyme family [13–16]. Their incredible success has spurred the development of many variations, including systems in which the pyrazolyl N groups have been replaced by sulfur donors. Such systems include thioether [17] and methimazolyl-containing [18–20] ligands. However, to our knowledge there are as yet no boron-based scorpionate ligands bearing a sulfur donor derived from an alkylthiolate group, most likely because of the synthetic difficulties of installing an alkylthiolate appendage. We have turned to a carbon-centered framework as a synthetically feasible alternative to the boron-centered systems. Herein we describe the coordination behavior of the scorpionate ligands L^1H and L^2H (Fig. 1). Both of these ligands rely on a central carbon atom in place of boron to link the imidazolyl and alkylthiolate donors into a tripodal framework [21]. The ligand L^1H was originally synthesized by Bosnich over 20 years ago for use in the preparation of models of blue copper proteins [22]. Still, little is known about its coordination chemistry, and to our knowledge no X-ray structures of complexes containing L^1 have been reported to date. The synthesis of the ligand L^2H was previously communicated by some of us [23].

We report here the first X-ray structure of any transition metal complex of the scorpionate ligand L^1 . In addition, the first iron(II) complex of L^2 has been synthesized and crystallographically characterized, and a new dinuclear zinc(II) complex of L^2 has been characterized by both 1H NMR spectroscopy and X-ray crystallography, allowing for a comparison between solution and solid-state structures. These different structures reveal that the L^1/L^2 framework can adopt three different coordination modes, including the expected tripodal N_2S bonding mode.

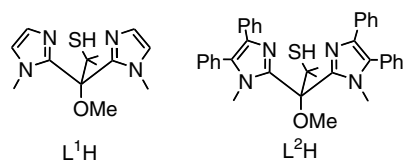


Fig. 1. Schematic presentation of the ligands.

2. Experimental

2.1. Materials and general methods

No special precautions were taken for the synthesis of **1**. All synthetic procedures for complexes **2** and **3** were carried out by using a dry-box or Schlenk techniques. For the synthesis of complex **3**, MeOH and CH_2Cl_2 were dried by refluxing over CaH_2 for 18 h and then distilled. Traces of oxygen were removed from these solvents by 3 cycles of freeze–pump–thaw. Ligands L^1H [22] and L^2H [23] were prepared as described in the literature. All other chemicals used in the experiments were of analytical grade from commercial sources and used without further purifications.

2.1.1. Synthesis of $[(L^1)_3Zn_3Br_2]Br$ (**1**)

Methanol (15 mL) was added to L^1H (0.050 g, 0.178 mmol), NaOMe (0.011 g, 0.196 mmol) and $ZnBr_2$ (0.044 g, 0.196 mmol) to yield a clear yellow solution. Overnight a white precipitate formed and the solution was filtered. This precipitate was dissolved by addition of 2 mL of hot CH_3CN . Crystals suitable for X-ray diffraction were obtained by diffusion of Et_2O into a CH_3CN solution of **1**. Yield <2%.

2.1.2. Synthesis of $[(L^2)_2Zn_2Br_2]$ (**2**)

To a solution of L^2H (0.1 g, 0.17 mmol) in CH_2Cl_2 (10 mL) was added NaOH (0.008 g, 0.19 mmol) in MeOH, and then the mixture was bubbled with argon for 30 minutes to make sure that the solution was oxygen-free. An amount of $ZnBr_2$ (0.039 g, 0.17 mmol) was dissolved in MeOH (5 mL) and bubbled with argon for 30 minutes. The methanolic solution of $ZnBr_2$ was added dropwise to the solution of deprotonated ligand and the reaction mixture was stirred for 18 h under argon. The complex **2** precipitated from the reaction mixture as a white powder, which was filtered, washed with Et_2O and dried under vacuum. Yield: 0.07 g, 56%. Crystals suitable for X-ray diffraction were obtained by diffusion of Et_2O into a CH_2Cl_2 solution of **2**. *Anal.* Calc. for $C_{74.5}H_{71}N_8O_2S_2Zn_2Br_2Cl[2 \cdot (CH_2Cl_2)_{0.5}]$: C, 59.63; H, 4.77; N, 7.47. Found: C, 59.40; H, 4.91; N, 7.29%. 1H NMR ($CDCl_3$, ppm): 7.56–7.11 (m, 40H, C_6H_5); 3.51 (s, 6H, N- CH_3); 3.26 (s, 6H, N- CH_3); 2.74 (s, 6H, O- CH_3); 1.93 (s, 12H, C- CH_3).

2.1.3. Synthesis of $(L^2)_2Fe$ (**3**)

A 2 mL solution of NaOH (0.009 g, 0.23 mmol) in MeOH was added to L^2H (0.06 g, 0.1 mmol) dissolved in CH_2Cl_2 (3 mL) and the mixture was stirred for 30 minutes. The solution of deprotonated ligand was then added to a solution of $FeCl_2$ (0.014 g, 0.11 mmol) in 3 mL MeOH, which was then stirred for 18 h to get a green precipitate. This precipitate was dissolved by addition of 2 mL CH_2Cl_2 to the reaction mixture. To the

resulting clear green solution, 3 mL of MeOH was added and colorless crystals were obtained by storing this solution at $-20\text{ }^{\circ}\text{C}$ for four days. Yield 0.03 g, 45%. IR of $3 \cdot (\text{CH}_3\text{OH})_2$ (KBr, cm^{-1}): 3479, 3051, 2975, 2915, 1603, 1504, 1463, 1443, 1367, 1262, 1229, 1179, 1125, 1075, 1027, 1001, 966, 930, 775, 697, 671, 648, 569, 530. For comparison the IR of L^2H is as follows (KBr, cm^{-1}): 3062, 2925, 1602, 1504, 1443, 1375, 1303, 1240, 1178, 1128, 1080, 1026, 964, 776, 698, 666, 627, 528. Anal. Calc. for $\text{C}_{76}\text{H}_{78}\text{N}_8\text{O}_4\text{S}_2\text{Fe}$ [$3 \cdot (\text{CH}_3\text{OH})_2$]: C, 70.90; H, 6.11; N, 8.70. Found: C, 71.35; H, 5.79; N, 8.97%.

2.2. Physical measurements

Elemental analyses were performed at Atlantic Microlab, Inc. (Norcross, GA). ^1H NMR spectrum in CDCl_3 was recorded on a Varian Unity Plus 400 spectrometer (400 MHz) at ambient probe temperature with tetramethylsilane as the internal reference. IR spectra were recorded on a Bruker Vector 22 IR spectrometer as KBr disks.

2.3. X-ray crystallography

Diffraction intensity data were collected with a Bruker Smart Apex CCD (**1** and **3**) and a SMART-1000 CCD (**2**) diffractometer with graphite monochromated Mo $\text{K}\alpha$ radiation. Crystal data, data collection, and refinement parameters for all structures are given in Table 1. The structures were solved using direct methods, completed by subsequent difference Fourier syntheses, and refined by full matrix least-squares procedures on F^2 . SADABS absorption corrections were applied to **1** and **3** (T_{min} , T_{max} = 0.390, 0.699 (**1**) and 0.898, 0.924 (**3**)). In the case of **2**, an analytical absorption correction was applied. Minimum and maximum transmission factors were 0.746 and 0.932, respectively. All non-hydrogen atoms were refined with anisotropic displacement coefficients, and hydrogen atoms were treated as idealized contributions in a riding group model.

In the crystal structure of **2** there is a disordered CH_2Cl_2 molecule. It was refined isotropically with occupancy factors of 0.125 for four chlorine atoms, 0.25

Table 1
Crystal data, data collection, and refinement parameters for **1–3**

Empirical formula	$\text{C}_{41}\text{H}_{60}\text{Br}_3\text{N}_{13}\text{O}_3\text{S}_3\text{Zn}_3(\mathbf{1} \cdot \text{CH}_3\text{CN})$	$\text{C}_{74.5}\text{H}_{69}\text{Br}_2\text{ClN}_8\text{O}_2\text{S}_2\text{Zn}_2[\mathbf{2} \cdot (\text{CH}_2\text{Cl}_2)_{0.5}]$	$\text{C}_{80}\text{H}_{94}\text{FeN}_8\text{O}_8\text{S}_2[\mathbf{3} \cdot (\text{CH}_3\text{OH})_6]$
Formula weight	1315.4	1498.56	1415.60
Temperature (K)	173(2)	153(2)	150(2)
Wavelength (Å)	0.71073	0.71073	0.71073
Crystal system	monoclinic	triclinic	triclinic
Space group	$P2_1/c$	$P(\bar{1})$	$P(\bar{1})$
<i>Unit cell dimensions</i>			
<i>a</i> (Å)	11.7069(7)	10.784(2)	11.0038(14)
<i>b</i> (Å)	22.4018(13)	11.371(2)	16.164(2)
<i>c</i> (Å)	20.4328(13)	29.455(4)	21.639(3)
α ($^{\circ}$)	90	97.326(3)	78.800(2)
β ($^{\circ}$)	104.721(1)	97.564(2)	88.549(2)
γ ($^{\circ}$)	90	96.209(3)	89.858(2)
Volume (Å ³)	5182.7(5)	3522.3(8)	3774.3(8)
<i>Z</i>	4	2	2
Density (calculated) (g cm ⁻³)	1.685	1.413	1.246
Absorption coefficient (mm ⁻¹)	3.862	1.967	0.315
<i>F</i> (000)	2656	1534	1504
Crystal size (mm)	0.30 × 0.20 × 0.10	0.17 × 0.15 × 0.04	0.35 × 0.30 × 0.25
θ Range for data collection ($^{\circ}$)	1.80–27.00	1.41–28.31	1.45–28.30
Index ranges	$-14 \leq h \leq 14$ $-28 \leq k \leq 26$ $-15 \leq l \leq 26$	$-13 \leq h \leq 13$ $-14 \leq k \leq 14$ $-37 \leq l \leq 39$	$-12 \leq h \leq 14$ $-21 \leq k \leq 19$ $-28 \leq l \leq 26$
Reflections collected	23055	32478	22764
Independent reflections	10738 [$R_{\text{int}} = 0.0467$]	16280 [$R_{\text{int}} = 0.044$]	16247 [$R_{\text{int}} = 0.0390$]
Absorption correction	SADABS	Analytical	SADABS
Refinement method	full-matrix least-squares on F^2	full-matrix least-squares on F^2	full-matrix least-squares on F^2
Data/restraints/parameters	10738/0/595	8660/0/839	16247/0/820
Goodness-of-fit on F^2	1.004	1.60	1.060
Final <i>R</i> indices [$I > 2\sigma(I)$] ^a	$R_1 = 0.0426$ $wR_2 = 0.1018$	$R_1 = 0.041$ $wR_2 = 0.088$	$R_1 = 0.1071$ $wR_2 = 0.3003$
<i>R</i> indices (all data) ^a	$R_1 = 0.0723$, $wR_2 = 0.1158$	$R_1 = 0.066$, $wR_2 = 0.097$	$R_1 = 0.1428$, $wR_2 = 0.3186$
Largest difference peak and hole (e Å ⁻³)	0.96 and -0.89	0.91 and -0.57	2.58 and -0.76

^a $R_1 = \sum ||F_o| - |F_c|| / \sum |F_o|$; $wR_2 = \left\{ \frac{\sum [w(F_o^2 - F_c^2)^2]}{\sum [w(F_o^2)^2]} \right\}^{1/2}$; $w = 1/[s^2(F_o^2) + (aP)^2 + bP]$; $P = [2F_c^2 + \max(F_o, 0)]/3$.

for two chlorine atoms and the occupancy factor of 0.5 for the carbon atom to give half a CH_2Cl_2 molecule per dimer unit while the remaining non-hydrogen atoms were refined anisotropically. Hydrogen atoms were included in idealized positions but not refined.

In the crystal structure of **3**, there are six MeOH solvent molecules. Two of those MeOH molecules are involved in weak hydrogen bonding with the thiolate sulfur atoms. The other four highly disordered MeOH molecules were treated as diffuse contributions with the SQUEEZE program (A. Spek, Platon software package). Corrections of the X-ray data by SQUEEZE found 159 e^- /unit cell which is close to the required value of 144 e^- /unit cell for four MeOH molecules. All samples of **3** examined diffracted weakly and diffusely, almost certainly a result of the loosely fixed solvent molecules, resulting in a rather high final *R* factor.

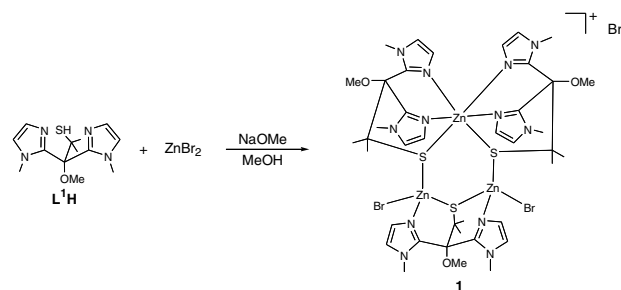
All software and sources of scattering factors for **1** and **3** are contained in the SHELXTL (5.10) program package (G. Sheldrick, Bruker XRD, Madison, WI). For **2** all calculations were performed using the TEXSAN crystallographic software package of Molecular Structure Corporation (TEXSAN for Windows version 1.05: Crystal Structure Analysis Package, Molecular Structure Corporation (1997–1998)).

3. Results and discussion

3.1. Synthesis of $[(L^1)_3Zn_3Br_2]Br$ (**1**)

The heteroscorpionate N_2S (thiolate) ligand L^1H , shown in Fig. 1, was originally prepared over 20 years ago for use in the synthesis of “blue copper” protein model complexes [22]. We recognized L^1 to be an intriguing example of a tripodal ligand with an alkylthiolate donor, which also had the added advantage of containing biomimetic imidazole donors. To our knowledge the blue copper modeling work was the only published account discussing L^1 , and there were as yet no crystallographically characterized compounds containing L^1 . As pointed out in the Introduction, heteroscorpionate ligands bearing an alkylthiolate donor are extremely rare, and thus we were compelled to see if we could develop the coordination chemistry of this system. We reacted L^1 with a Zn(II) source to determine its coordination behavior with this ion, and obtained a trinuclear zinc complex in which L^1 displays two distinct bonding modes.

For the synthesis of $[(L^1)_3Zn_3Br_2]Br$ (**1**), the three starting materials L^1H , NaOMe, and ZnBr_2 are dissolved together in MeOH, as shown in Scheme 1. The ligand L^1H is freely soluble in MeOH, unlike L^2H , and therefore the use of CH_2Cl_2 can be avoided, in contrast to the synthesis of **2** and **3** (vide infra). Initially a clear solution is obtained, but after 18 h a small amount of



Scheme 1.

white precipitate is formed and isolated by filtration. This solid has limited solubility, but can be redissolved in hot CH_3CN . From $\text{Et}_2\text{O}/\text{CH}_3\text{CN}$ a very small amount of **1** can be obtained as X-ray quality crystals. Attempts to scale up the reaction or obtain subsequent crops of **1** led to the formation of yellow oils or solids which could not be re-crystallized to give more **1**. Thus the yield of **1** is extremely low, and sometimes no crystals of **1** form, but the few crystals that were obtained by this method were utilized for X-ray crystallography. The low yield of **1** precluded us from obtaining other characterization data on **1**.

3.2. Crystal structure of $[(L^1)_3Zn_3Br_2]Br$ (**1**)

An ORTEP view of **1** is shown in Fig. 2. Crystallographic data are summarized in Table 1. Selected bond distances and angles are given in Table 2. Structural characterization of **1** has revealed a trinuclear zinc complex that crystallizes in the monoclinic space group $P2_1/c$. The metal:ligand ratio is 1:1, but the overall structure is much less symmetric than the simple formula

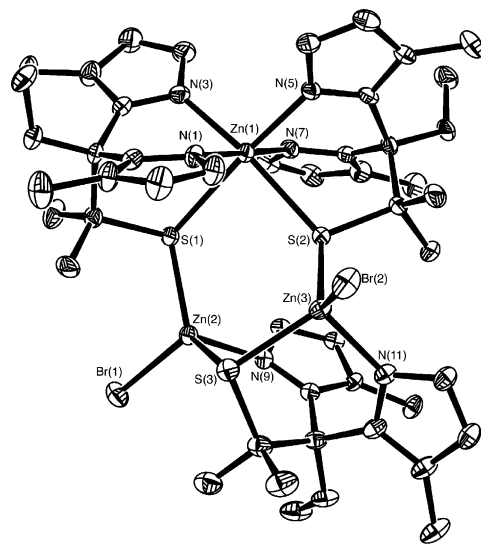


Fig. 2. Thermal ellipsoid plot of the cation of **1** at 40% probability. Hydrogen atoms are omitted for clarity.

Table 2
Bond lengths (Å) and angles (°) for **1**

<i>Bond lengths</i>	
Zn(1)–S(1)	2.6697(11)
Zn(1)–S(2)	2.5110(12)
Zn(1)–N(1)	2.091(3)
Zn(1)–N(3)	2.068(4)
Zn(1)–N(5)	2.055(3)
Zn(1)–N(7)	2.141(3)
Zn(2)–Br(1)	2.4371(7)
Zn(2)–S(1)	2.3115(12)
Zn(2)–S(3)	2.3575(12)
Zn(2)–N(9)	2.026(3)
Zn(3)–Br(2)	2.3931(6)
Zn(3)–S(2)	2.2843(11)
Zn(3)–S(3)	2.3715(12)
Zn(3)–N(11)	2.034(4)
<i>Bond angles</i>	
N(5)–Zn(1)–N(3)	99.28(14)
N(5)–Zn(1)–N(1)	98.94(14)
N(3)–Zn(1)–N(1)	84.15(14)
N(5)–Zn(1)–N(7)	83.42(13)
N(3)–Zn(1)–N(7)	93.26(14)
N(1)–Zn(1)–N(7)	176.73(14)
N(5)–Zn(1)–S(2)	88.92(10)
N(3)–Zn(1)–S(2)	169.75(10)
N(1)–Zn(1)–S(2)	100.75(10)
N(7)–Zn(1)–S(2)	81.50(10)
N(5)–Zn(1)–S(1)	175.56(11)
N(3)–Zn(1)–S(1)	84.21(10)
N(1)–Zn(1)–S(1)	84.11(10)
N(7)–Zn(1)–S(1)	93.66(9)
S(2)–Zn(1)–S(1)	87.33(4)
N(9)–Zn(2)–S(1)	108.76(10)
N(9)–Zn(2)–S(3)	90.86(10)
S(1)–Zn(2)–S(3)	123.06(4)
N(9)–Zn(2)–Br(1)	100.78(9)
S(1)–Zn(2)–Br(1)	108.29(4)
S(3)–Zn(2)–Br(1)	119.96(3)
N(11)–Zn(3)–S(2)	107.90(10)
N(11)–Zn(3)–S(3)	99.86(11)
S(2)–Zn(3)–S(3)	109.06(4)
N(11)–Zn(3)–Br(2)	103.06(10)
S(2)–Zn(3)–Br(2)	121.46(4)
S(3)–Zn(3)–Br(2)	112.93(3)

implies. The ligands exhibit two distinct coordination modes. One of the zinc centers, Zn(1), is bound by two ligands each through the expected tripodal N₂S coordination. The geometry at this zinc center is best described as distorted octahedral with *cis* angles ranging from 83° to 101° and *trans* angles ranging from 170° to 177°. The two sulfur atoms are in a *cis* arrangement. The Zn(1)–N(im) distances range from 2.055(3) to 2.141(3) Å. In the case of the longer Zn(1)–N(im) distances (Zn(1)–N(7) = 2.141(3) Å and Zn(1)–N(1) = 2.091(3) Å), the imidazoles are *trans* to one another, while the imidazoles with shorter bond distances (Zn(1)–N(5) = 2.055(3) Å and Zn(1)–N(3) = 2.068(4) Å) are *trans* to the sulfur atoms. From these distances it is reasonable to conclude that N(7) and N(1) lie on axial positions while N(5) and N(3) lie on equatorial positions in the distorted octahe-

dral geometry. All of these Zn–N(im) distances are reasonable compared to other octahedral zinc complexes containing imidazole donors [24,25]. Interestingly, the Zn(1)–S distances of Zn(1)–S(1) = 2.6697(11) Å and Zn(1)–S(2) = 2.5110(12) Å are quite long for a typical Zn–S bond, and considerably longer than the distances from the thiolate sulfur atoms to the respective tetrahedral zinc(II) ions: Zn(2)–S(1) 2.3115(12) Å and Zn(3)–S(2) 2.2843(11) Å. This observation is counterintuitive to the expectation that the Zn–S bonds of the chelate ring should be shorter than the bridging Zn–S bonds. However, this same trend is observed for two other trinuclear zinc complexes, [(MBPA)₄Zn₃]₂ (MBPAH = *N*-(2-mercaptoisobutyl)-(picolyl)amine) [26] and [Zn{Zn(L³)₂}₂](ClO₄)₂ (L³ = 2-[(2-pyridylmethyl)amino]ethanethiolate) [27], both of which have 6-coordinate and 4-coordinate zinc(II) ions bridged by thiolate ligands. In these compounds the sulfur distance to the six-coordinate zinc ion is significantly longer than the sulfur distance to the four-coordinate zinc center ([(MBPA)₄Zn₃]₂: Zn_{octahedral}–S = 2.545(3) Å, Zn_{tetrahedral}–S = 2.365(3) Å; [Zn{Zn(L³)₂}₂](ClO₄)₂: Zn_{octahedral}–S = 2.538(3)–2.596(3) Å, Zn_{tetrahedral}–S = 2.346(3)–2.363(3) Å). In both of the latter complexes the thiolate donor is also part of a chelate ring that includes the octahedral zinc ion. The considerably longer Zn_{octahedral}–S distances are likely a consequence of the increase in coordination number compared to a tetrahedral zinc site.

The tetrahedral zinc centers Zn(2) and Zn(3) are not only bridged by sulfur atoms to the octahedral zinc ion, but are also connected to each other by the thiolate arm of a third ligand. Each of these four-coordinate zinc ions is also bound by a separate imidazole donor from the same ligand. Thus the imidazolyl groups together with the bridgehead carbon atom also participate in bridging the dinuclear zinc fragment. This (im)–C(im)–type bridge has been observed previously for the related N₃ scorpionate ligand tris[2-(1-methylimidazolyl)methoxymethane (timm)], which has three imidazolyl donors connected by a central C₃ symmetric carbon atom. The dimeric complexes of formula [Cu(timm)₂][BF₄]₂ [28] and [Pd₂Cl₂(timm)₂]₂Cl₂ [29] have structures which show the ligand bound to one metal ion through two imidazole rings while the third imidazole group coordinates to the other metal ion of the dimer. Interestingly, the unusual “1 + 2” assembly of an octahedral zinc ion bridged to a dinuclear fragment of two tetrahedral zinc ions has been seen before for another N₂S(thiolate) scorpionate ligand, but in this case the tetrahedral zinc ions are bridged by a (PhO)₂PO₂[−] ligand [21b]. The fourth site of each distorted tetrahedral zinc center in **1** is occupied by a bromide ion. The Zn–N(im) distances for the four-coordinate zinc sites are 2.026(3) and 2.034(4) Å. These Zn–N lengths are slightly shorter than those found for the octahedral zinc site, as to be expected from the lower coordination number of the

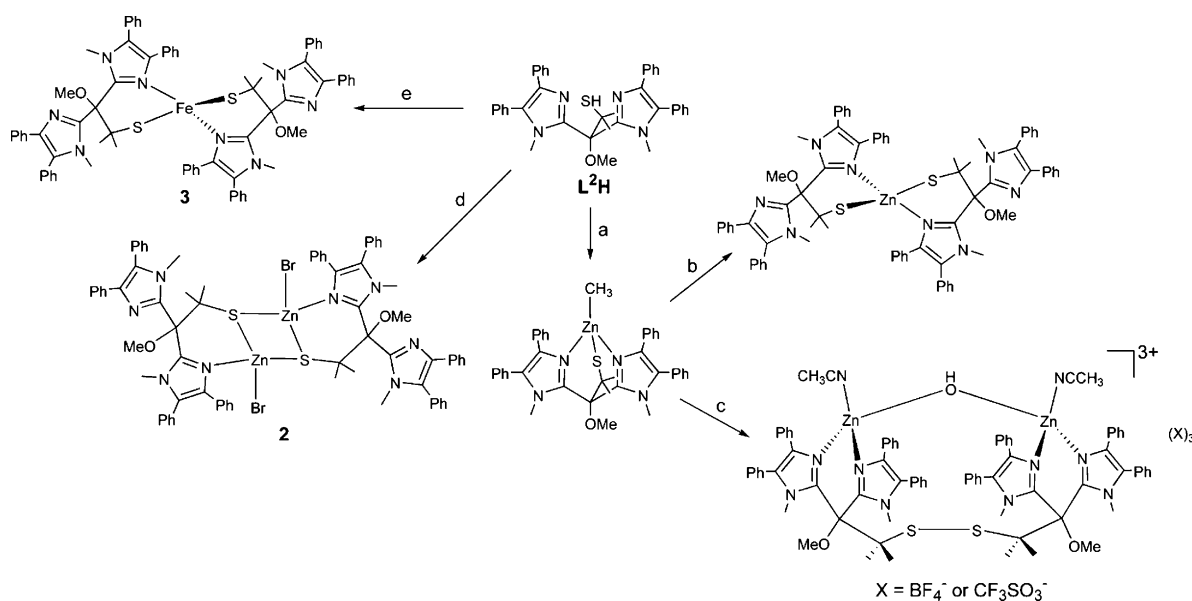
tetrahedral centers. The angles around the two four-coordinate zinc ions are distinct, ranging from 90.9° – 123.1° for Zn(2) to 99.9° – 121.5° for Zn(3), making them both rather distorted from ideal tetrahedral geometry.

3.3. Coordination behavior of L^2

Although L^1 exhibited the desired tripodal bonding mode in complex **1**, it also demonstrated a propensity to form both 2:1 octahedral complexes as well as thiolate-bridged oligomers. Given these results, we sought methods for synthetically modifying L^1 to incorporate steric bulk near the metal center during tripodal coordination, thereby favoring monomeric $(N_2S)ZnL$ complexes. Modification of the imidazole groups was the most synthetically feasible method of achieving this goal given the stepwise synthesis of L^1H [22], and thus we targeted the diphenyl-substituted analog L^2H , shown in Fig. 1. The synthesis of L^2H has been communicated previously, and in the same work L^2 was shown to react with $Zn(CH_3)_2$ to give the neutral, monomeric zinc alkyl complex $(L^2)ZnCH_3$, as seen in Scheme 2 [23]. The synthesis of this complex demonstrated that L^2 coordinates in the desired tridentate facial mode to give a tetrahedral $(N_2S)ZnL$ complex. This complex was prepared as a possible starting material for the formation of $(L^2)ZnOH$ by reaction with water. However, upon reaction of $(L^2)ZnCH_3$ with water in toluene, a redistribution of ligand:metal stoichiometry took place along with a rearrangement of the N_2S bonding mode of L^2 to a bidentate N,S mode, resulting in the formation of a four-coordinate N_2S_2 –Zn complex. Alternatively, if $(L^2)ZnCH_3$ was reacted under acidic conditions (HBF_4 or CF_3SO_3H in

CH_3CN), the rearranged Zn – N_2S_2 product was not obtained, but instead the dinuclear complexes $[(L^2)_2Zn_2(CH_3CN)_2(\mu-OH)](X)_3$ ($X = BF_4^-$, $CF_3SO_3^-$) were isolated and crystallographically characterized [23]. During the formation of these dimers an undesirable intramolecular disulfide linkage had formed. These synthetic observations are summarized in Scheme 2.

In continuing our efforts to determine the coordination behavior of L^2 , we have reacted L^2 with the metal salts $ZnBr_2$ and $FeCl_2$, as shown in Scheme 2. The syntheses of **2** and **3** were carried out under the strict exclusion of air to prevent the possible oxidation of the thiolate ligand to a disulfide and in the case of **3**, to prevent oxidation of the Fe(II) product. The ligand L^2H is freely soluble in CH_2Cl_2 but only sparingly soluble in MeOH. Thus, L^2H was first dissolved in CH_2Cl_2 and then deprotonated by the addition of NaOH in MeOH in the synthesis of both **2** and **3**. For **2**, a solution of $ZnBr_2$ in MeOH was added dropwise to the solution of L^2 whereas for **3** the addition was reversed and ligand was added to metal. Complex **2** precipitates from the reaction mixture as a white powder. After workup this powder was shown to be pure **2** by its 1H NMR spectrum. Complex **2** is freely soluble in CH_2Cl_2 , and recrystallization of **2** from vapor diffusion of Et_2O into CH_2Cl_2 gave the crystals that were used for the structural determination. In the case of **3**, a precipitate also forms in the reaction mixture, but this precipitate is not isolated and instead is simply recrystallized directly by the addition of CH_2Cl_2 to the reaction mixture to redissolve the solid. X-ray quality crystals of **3** are obtained after storage of this mixture at $-20^\circ C$.



Scheme 2. Conditions: (a) 1.4 $Zn(CH_3)_2$, toluene, rt, 3 h. (b) 30 H_2O , toluene, rt, 6 d. (c) 2 HBF_4 (aq.) or 2 CF_3SO_3H , CH_3CN , rt, 24 h. (d) 1.1 NaOH, MeOH; 1 $ZnBr_2$, MeOH; 18 h. (e) 2.2 NaOH, MeOH; 1.1 $FeCl_2$, MeOH; 18 h.

3.4. Crystal structure of $[(L^2)_2Zn_2Br_2]$ (**2**)

An ORTEP view of **2** is shown in Fig. 3. Crystallographic data are summarized in Table 1. Selected bond distances and angles are given in Table 3. Complex **2** crystallizes in the triclinic $P(\bar{1})$ space group. The dimer does not sit on an inversion center, and therefore all bonds and angles are crystallographically unique. A CH_2Cl_2 molecule of 1/2 occupancy was located per dimeric unit. Both zinc centers have a distorted tetrahedral geometry and are bridged by two sulfur atoms from two ligand molecules to give a Zn_2S_2 rhomb. In addition to the bridging thiolates, a nitrogen atom from one of the *N*-methyl-4,5-diphenylimidazole rings coordinates each

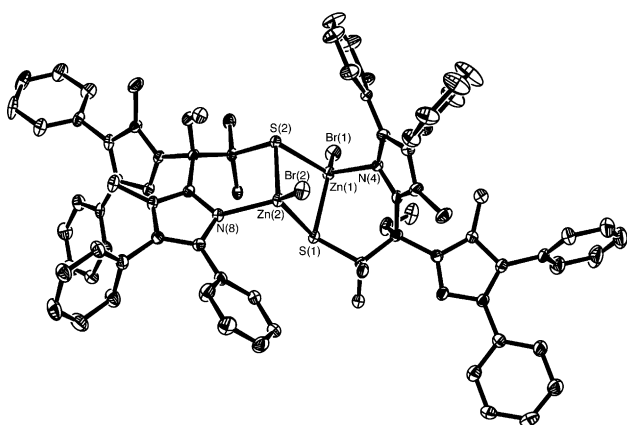


Fig. 3. Thermal ellipsoid plot of **2** at 40% probability. Hydrogen atoms are omitted for clarity.

Table 3
Bond lengths (Å) and angles (°) for **2**

Bond lengths	
Br(1)–Zn(1)	2.3706(9)
Br(2)–Zn(2)	2.3573(9)
Zn(1)–S(1)	2.3400(13)
Zn(1)–S(2)	2.3807(13)
Zn(1)–N(4)	2.061(3)
Zn(2)–S(1)	2.4034(13)
Zn(2)–S(2)	2.3787(13)
Zn(2)–N(8)	2.050(4)
Bond angles	
Br(1)–Zn(1)–S(1)	114.89(4)
Br(1)–Zn(1)–S(2)	122.77(4)
Br(1)–Zn(1)–N(4)	111.00(9)
S(1)–Zn(1)–S(2)	94.84(4)
S(1)–Zn(1)–N(4)	99.19(10)
S(2)–Zn(1)–N(4)	110.77(10)
Br(2)–Zn(2)–S(1)	113.12(4)
Br(2)–Zn(2)–S(2)	129.23(4)
Br(2)–Zn(2)–N(8)	117.78(10)
S(1)–Zn(2)–S(2)	93.25(4)
S(1)–Zn(2)–N(8)	104.66(10)
S(2)–Zn(2)–N(8)	94.06(10)
Zn(1)–S(1)–Zn2	82.92(4)
Zn(1)–S(2)–Zn(2)	82.59(4)

zinc atom. A bromide ion completes the coordination sphere of each zinc atom. Each ligand has one imidazole moiety that is free and not coordinated to a zinc atom, and thus each ligand binds in a bidentate N,S fashion through one nitrogen atom and one μ -sulfur atom. As pointed out in Section 3.3, evidence for this type of bonding mode has been obtained previously for L^2 . In comparison, the dimeric complexes of the N_3 scorpionate ligand timm, $[Cu(timm)_2][BF_4]_2$ [28] and $[Pd_2Cl_2(timm)_2]Cl_2$ [29], described previously in Section 3.2, have structures which show a bidentate N,N bonding mode. Thus, the bidentate bonding mode of these carbon-centered scorpionate ligands is not unique to mixed N/S systems, and is seen for the homoleptic N_3 systems as well.

The Zn–S distances of **2** range between 2.3400(13) and 2.4034(13) Å, which is within the range of other $Zn_2(\mu-SR)_2$ complexes [30–34], such as the homoleptic complex $[(Et_4N)_2Zn_2(SET)_6]$ [33] where $d(Zn-S) = 2.394(1)$ and $2.456(1)$ Å, or $[Zn_2(CH_3)_2(\{SC_6H_4(R)-CH(Me)NMe_2\}-2)]_2$, where the zinc ions are bound by an N,S chelate ring and $d(Zn-S)$ ranges between 2.389(1) and 2.453(2) Å [34]. The carbon atoms attached to each thiolate bridge are on opposite sides of the Zn_2S_2 plane, as are the bromine atoms, and thus **2** can be classified in the *anti* form [33]. The Zn(1)–N(4) and Zn(2)–N(8) distances of 2.061(3) and 2.050(4) Å, respectively, are close to other $Zn_{tetrahedral}-N_{imidazole}$ distances [35–37]. The Zn–Br distances of 2.3573(9) and 2.3706(9) Å are also unexceptional [9,35,38]. The angles around the zinc centers range from 82.59(4)°–129.23(4)°, which indicates a significant distortion from tetrahedral geometry. The dihedral angle between the two planes defined by Zn(1)S₂ and Zn(2)S₂ is 19.3°, giving a slight V shape to the Zn_2S_2 unit. In the literature this dihedral angle is found to vary from 0° for $[(Et_4N)_2Zn_2(SET)_6]$ [33] to 29.18° for $[(Me)Zn(SBu^t)(cis-C_6H_{15}N_3)]_2$ where $(cis-C_6H_{15}N_3) = 1,3,5$ -trimethylhexahydro-1,3,5-triazine [39]. The reasons for the variance in this fold angle are not clear. The distance between the two zinc atoms in **2** is 3.141 Å which is also in the normal range for $Zn_2(\mu-SR)_2$ complexes [33].

3.5. 1H NMR spectrum of $[(L^2)_2Zn_2Br_2]$ (**2**)

The 1H NMR spectrum for **2** in $CDCl_3$ provides good evidence that the dinuclear structure obtained from X-ray crystallography remains intact in solution. The resonances for the phenyl protons of **2** appear as a complex multiplet in the region δ 7.11–7.56 ppm, and do not provide much structural information. However, for the N–CH₃ substituents, two distinct singlets are observed at 3.51 and 3.26 ppm, consistent with the two different types of imidazole groups in the dimer. We assign the upfield peak at 3.26 ppm to the non-coordinated imidazole group, whereas the peak at 3.51 ppm is assigned to

the imidazole group bound to the zinc(II) ion. The latter assignment is based on the ^1H NMR spectra for $(\text{L}^2)\text{ZnCH}_3$ and $[(\text{L}^2)_2\text{Zn}_2(\text{CH}_3\text{CN})_2(\mu\text{-OH})](\text{X})_3$ ($\text{X} = \text{BF}_4^-, \text{CF}_3\text{SO}_3^-$), both of which have only the coordinated type of imidazolyl group (Scheme 2) and exhibit downfield-shifted N–CH₃ resonances of δ 3.87 and 3.95 ppm, respectively [23]. A similar pattern to that of **2** was seen for $(\text{L}^2)_2\text{Zn}$, which exhibited two peaks at 2.95 and 3.87 ppm, presumed to be the free and bound imidazole groups, respectively [23]. Curiously, the free ligand itself, L^2H , gives rise to a relatively downfield N–CH₃ resonance of 3.53 ppm. However, the precedent for a coordinated N–CH₃ peak being significantly downfield-shifted is clear from the former data. The singlet at 2.74 ppm in the spectrum of **2** is assigned to the O–CH₃ resonance, which is close to the same peak found for $(\text{L}^2)_2\text{Zn}$ (O–CH₃: δ 2.57 ppm), yet quite distinct from that of $(\text{L}^2)\text{ZnCH}_3$ (3.57 ppm) or $[(\text{L}^2)\text{Zn}(\mu\text{-OH})\text{-Zn}(\text{L}^2)]^{3+}$ (3.56 ppm). Finally, the gem-dimethyl protons for **2** appear as a singlet at δ 1.93 ppm, which is downfield of the same resonance found for the free ligand L^2H (1.60 ppm) or for $(\text{L}^2)\text{ZnCH}_3$ (1.64 ppm), in which L^2 is bound in a tripodal mode. Thus the ^1H NMR spectrum of **2** appears to be quite characteristic of the bonding mode of L^2 (N,S versus N,N,S for $(\text{L}^2)\text{ZnCH}_3$ and N,N for $[(\text{L}^2)\text{Zn}(\mu\text{-OH})\text{-Zn}(\text{L}^2)]^{3+}$).

3.6. Crystal structure of $(\text{L}^2)_2\text{Fe}$ (**3**)

An ORTEP view of **3** is shown in Fig. 4. Crystallographic data are summarized in Table 1. Selected bond distances and angles are given in Table 4. This complex crystallizes in the triclinic space group $P(\bar{1})$. The ferrous ion adopts a distorted tetrahedral geometry and is coordinated by two ligand molecules through one imidazole and one thiolate donor, which makes the complex neutral in charge. As observed in the case of **2**, the other imidazole donor from each ligand molecule remains uncoordinated, demonstrating the preference for an N,S binding mode over an N₂S mode for L^2 . The two MeOH molecules found in the lattice appear to be involved in hydrogen bonding with separate thiolate sulfur atoms.

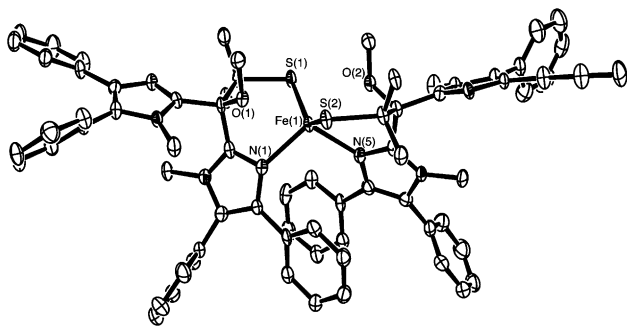


Fig. 4. Thermal ellipsoid plot of **3** at 40% probability. Hydrogen atoms are omitted for clarity.

Table 4
Bond lengths (Å) and angles (°) for **3**

Bond lengths	
Fe(1)–N(1)	2.157(4)
Fe(1)–N(5)	2.157(4)
Fe(1)–S(2)	2.3363(14)
Fe(1)–S(1)	2.3480(14)
Bond angles	
N(1)–Fe(1)–N(5)	102.77(15)
N(1)–Fe(1)–S(2)	107.65(11)
N(5)–Fe(1)–S(2)	99.65(11)
N(1)–Fe(1)–S(1)	98.68(10)
N(5)–Fe(1)–S(1)	109.78(11)
S(2)–Fe(1)–S(1)	134.72(6)

The hydrogen atoms on the MeOH molecules could not be located by X-ray diffraction, but the distances between the oxygen and sulfur atoms, O(1S)–S(1) = 3.183 Å and O(2S)–S(2) = 3.167 Å, indicate an H-bonding interaction [40]. Despite these putative hydrogen bonds, the Fe–S distances of Fe–S(1) = 2.3480(14) Å and Fe–S(2) = 2.3363(14) Å, are quite normal. Interestingly, both the methoxy oxygen atoms of the ligands are oriented towards the iron(II) ion, with distances of Fe–O(1) = 2.462 and Fe–O(2) = 2.473 Å. These distances are comparable to other Fe–O(ether) distances for compounds in which an Fe–O(ether) bond has been assigned. For example, a mean Fe–O distance of 2.40 Å is found for the crown ether complex $\{[\text{Fe}(\text{12-crown-4})_2](\text{PF}_6)_2\}$ [41], and $(\text{Fe–O})_{\text{ave}} = 2.386(3)$ Å for the calixarene complex $[\text{Fe}(\text{II–H})(\text{FeCl}_4)_2]$ [42] [(II–H) = 5,11,17,23-tetra-*tert*-butyl-24-hydroxy-26,27,28-tris(diethyl-carbamoylmethoxy)calix-[4]arene]. These data suggest that there is a bonding interaction between the Fe^{2+} ion and the methoxy oxygen atoms, and the ligand has adopted the unexpected tripodal N₂O bonding mode. However, the angles do not support an assignment of octahedral geometry in preference to a distorted tetrahedral geometry, and therefore we conclude that this O(ether)–Fe^{II} interaction is weak at best. The Fe–N distances of 2.157(4) Å are slightly longer than the bond length of 2.095(4) Å for the related $\text{Fe}^{\text{II}}(\text{N}_2\text{S}_2)$ complex $\text{Fe}(\text{S-2,6-}i\text{-Pr}_2\text{C}_6\text{H}_3)_2(1\text{-MeIm})_2$ [43]. The X-ray structures of complexes **2** and **3** together with the synthesis and spectroscopic characterization of $(\text{L}^2)_2\text{Zn}$ (Scheme 2) make it clear that L^2 has a particular preference for coordination via a bidentate N,S bonding mode.

4. Conclusions

We have succeeded in obtaining the first X-ray structure of a transition metal complex of the N₂S(thiolate) ligand L^1 . This trinuclear zinc complex **1** showed that L^1 does bind in the designed tripodal mode, but also exhibits another multibringing bonding mode involving bridging imidazole and thiolate groups. The

ligand L^2 is a modified version of L^1 bearing phenyl substituents, and exhibits a third type of bidentate N,S bonding mode evidenced by the X-ray structures of the dinuclear zinc(II) complex **2** and the mononuclear iron(II) complex **3**. This bonding mode is likely favored in the case of L^2 because of a combination of strain around the central carbon atom and the weakened donor power of the imidazole groups caused by the electron-withdrawing phenyl substituents. In addition, yet another type of bonding mode may be operative in **3**; there is some evidence for a weak bond between the methoxy oxygen atom of L^2 and Fe(II), giving rise to tripodal NSO(ether)-type coordination. Clearly, further modifications to these heteroscorpionate N_2S (thiolate) ligands are necessary before they can rival the tris(pyrazolyl)borates in terms of their ability to enforce a biologically relevant monomeric, tetrahedral geometry at the metal center. The results obtained here suggest that replacing the phenyl substituents with electron-donating groups (e.g. alkyl groups), as well as increasing the steric encumbrance near the sulfur atom to discourage thiolate bridges from forming, should favor complexes of the desired nuclearity and geometry.

5. Supplementary material

The X-ray crystallographic files, in CIF format, have been deposited with the Cambridge Crystallographic Data Center, CCDC Nos. 213062, 213475 and 211497 for **1**, **2**, and **3**, respectively. Copies of this information may be obtained from The Director, CCDC, 12 Union Road, Cambridge, CB2 1EZ, UK, (fax: +44-1223-336033; email: deposit@ccdc.cam.ac.uk or [www: http://www.ccdc.cam.ac.uk/conts/retrieving.html](http://www.ccdc.cam.ac.uk/conts/retrieving.html)) on request, quoting the deposition number.

Acknowledgements

The authors wish to acknowledge the National Institutes of Health (GM 62309) for financial support. D.P.G. is also grateful for an Alfred P. Sloan, Jr. Research Fellowship.

References

- [1] N. Borkakoti, *J. Mol. Med.* 78 (2000) 261.
- [2] C.O. Pabo, E. Peisach, R.A. Grant, *Annu. Rev. Biochem.* 70 (2001) 313.
- [3] R. Meijers, R.J. Morris, H.W. Adolph, A. Merli, V.S. Lamzin, E.S. Cedergren-Zeppezauer, *J. Biol. Chem.* 276 (2001) 9316.
- [4] H.W. Park, S.R. Boduluri, J.F. Moomaw, P.J. Casey, L.S. Beese, *Science* 275 (1997) 1800, and references therein.
- [5] M.H. Bracey, J. Christiansen, P. Tovar, S.P. Cramer, S.G. Bartlett, *Biochemistry* 33 (1994) 13126, and references therein.
- [6] D.W. Randall, D.R. Gamelin, L.B. LaCroix, E.I. Solomon, *J. Biol. Inorg. Chem.* 5 (2000) 16.
- [7] W. Huang, J. Jia, J. Cummings, M. Nelson, G. Schneider, Y. Lindqvist, *Structure* 5 (1997) 691.
- [8] (a) P.T.R. Rajagopalan, S. Grimme, D. Pei, *Biochemistry* 39 (2000) 779;
(b) T. Meinnel, C. Lazennec, S. Blanquet, *J. Mol. Biol.* 254 (1995) 175.
- [9] S. Chang, V.V. Karambelkar, R.C. diTargiani, D.P. Goldberg, *Inorg. Chem.* 40 (2001) 194.
- [10] S. Chang, V.V. Karambelkar, R.D. Sommer, A.L. Rheingold, D.P. Goldberg, *Inorg. Chem.* 41 (2002) 239.
- [11] S. Chang, R.D. Sommer, A.L. Rheingold, D.P. Goldberg, *Chem. Commun.* (2001) 2396.
- [12] R.C. diTargiani, S. Chang, M.H. Salter Jr., R.D. Hancock, D.P. Goldberg, *Inorg. Chem.* 42 (2003) 5825.
- [13] S. Trofimenko, *Scorpionates – The Coordination Chemistry of Polypyrazolylborate Ligands*, Imperial College Press, River Edge, NJ, 1999.
- [14] G. Parkin, *Chem. Commun.* (2000) 1971.
- [15] R. Alsfasser, S. Trofimenko, A. Looney, G. Parkin, H. Vahrenkamp, *Inorg. Chem.* 30 (1991) 4098.
- [16] N. Kitajima, S. Hikichi, M. Tanaka, Y. Moro-oka, *J. Am. Chem. Soc.* 115 (1993) 5496.
- [17] S.J. Chiou, J. Innocent, C.G. Riordan, K.C. Lam, L. Liable-Sands, A.L. Rheingold, *Inorg. Chem.* 39 (2000) 4347.
- [18] M. Garner, J. Reglinski, I. Cassidy, M.D. Spicer, A.R. Kennedy, *Chem. Commun.* (1996) 1975.
- [19] J. Reglinski, M. Garner, I.D. Cassidy, P.A. Slavin, M.D. Spicer, D.R. Armstrong, *J. Chem. Soc., Dalton Trans.* (1999) 2119.
- [20] C. Kimblin, T. Hascall, G. Parkin, *Inorg. Chem.* 36 (1997) 5680.
- [21] (a) For a related heteroscorpionate $N_2S_{thiolate}$ ligand see B.S. Hammes, C.J. Carrano, *Inorg. Chem.* 40 (2001) 919;
(b) B.S. Hammes, C.J. Carrano, *J. Chem. Soc., Dalton Trans.* (2000) 3304;
(c) B.S. Hammes, C.J. Carrano, *Chem. Commun.* (2000) 1635.
- [22] J.M. Downes, J. Whelan, B. Bosnich, *Inorg. Chem.* 20 (1981) 1081.
- [23] V.V. Karambelkar, D. Krishnamurthy, C.L. Stern, L.N. Zakharov, A.L. Rheingold, D.P. Goldberg, *Chem. Commun.* (2002) 2772.
- [24] T.A. Zevaco, H. Görls, E. Dinjus, *Inorg. Chim. Acta* 269 (1998) 283.
- [25] N. Niklas, O. Walter, F. Hampel, R. Alsfasser, *J. Chem. Soc., Dalton Trans.* (2002) 3367.
- [26] U. Brand, H. Vahrenkamp, *Inorg. Chim. Acta* 308 (2000) 97.
- [27] M. Mikuriya, X. Jian, S.I. Ikemi, T. Kawahashi, H. Tsutsumi, *Bull. Chem. Soc. Jpn.* 71 (1998) 2161.
- [28] T.N. Sorrell, A.S. Borovik, *J. Am. Chem. Soc.* 109 (1987) 4255.
- [29] T. Rütther, M.C. Done, K.J. Cavell, E.J. Peacock, B.W. Skelton, A.H. White, *Organometallics* 20 (2001) 5522.
- [30] W.P. Chung, J.C. Dewan, M.A. Walters, *Inorg. Chem.* 30 (1991) 4280.
- [31] B. Kaptein, L. Wang-Griffin, G. Barf, R.M. Kellogg, *Chem. Commun.* (1987) 1457.
- [32] K.S. Anjali, J.J. Vittal, *Main Group Metal Chemistry* 24 (2001) 129.
- [33] A.D. Watson, C.P. Rao, J.R. Dorfman, R.H. Holm, *Inorg. Chem.* 24 (1985) 2820.
- [34] D.M. Knotter, M.D. Janssen, D.M. Grove, W.J.J. Smeets, E. Horn, A.L. Spek, G. van Koten, *Inorg. Chem.* 30 (1991) 4361.
- [35] R.J. Read, M.N.G. James, *Acta Cryst.* B36 (1980) 3100.
- [36] B. Müller, A. Schneider, M. Tesmer, H. Vahrenkamp, *Inorg. Chem.* 38 (1999) 1900.
- [37] W. Kläui, C. Piefer, G. Rheinwald, H.R. Lang, *Eur. J. Inorg. Chem.* (2000) 1549.

- [38] N. Galván-Tejada, S. Bernès, S.E. Castillo-Blum, H. Nöth, R. Vicente, N. Barba-Behrens, *J. Inorg. Biochem.* 91 (2002) 339.
- [39] M.A. Malik, M. Motevalli, J.R. Walsh, P. O'Brien, A.C. Jones, *J. Mater. Chem.* 5 (1995) 731.
- [40] M. Rombach, H. Vahrenkamp, *Inorg. Chem.* 40 (2001) 6144.
- [41] K. Meier, G. Rihs, *Angew. Chem. Intl. Ed. Engl.* 24 (1985) 858.
- [42] M.I. Ogden, B.W. Skelton, A.H. White, *J. Chem. Soc., Dalton Trans.* (2001) 3073.
- [43] C.E. Forde, A.J. Lough, R.H. Morris, R. Ramachandran, *Inorg. Chem.* 35 (1996) 2747.